

Accurate Angle Estimation in Smart Knee Prostheses via Magnetic Implantable and Skin-mounted Sensors

Arash Arami, Arnaud Barré and Kamiar Aminian

Laboratory of Movement Analysis and Measurement

Ecole Polytechnique Fédérale de Lausanne (EPFL), Switzerland, e-mail: kamiar.aminian@epfl.ch, <http://lmam.epfl.ch>

SUMMARY

In this work we investigated how to measure concurrently flexion-extension and internal-external rotations in a smart knee prosthesis. A configuration of magnetic sensors and magnets were designed and embedded in knee prostheses in which each sensor measures a mixture of information related to both rotations. Using correlation analyses, angle estimators were designed to separate the flexion-extension and internal-external rotations information. The estimators were validated in a mechanical knee simulator towards a reference system. The effect of imposed abduction-adduction was also analyzed on the estimations performances. To reduce the power consumption of the internal system, we reduced the sampling rate and duty cycled the sensors and compensated the lack of information with skin-mounted sensors on four subjects. The fusion between implantable and skin-mounted sensors drastically improved the flexion-extension angle estimation, but not the internal-external estimation.

INTRODUCTION

There are a few instrumented knee prostheses which are mainly designed for force measurements [1,2] while measurement of kinematics of the prosthesis was left to be done by skin-mounted sensors or marker-based systems which suffer from soft tissue artifact (STA) [3].

Recently we introduced the general concept of an instrumented prosthesis including sensors, electronics, wireless communication and remote powering for in-vivo force and kinematics measurements [4]. Different magnetic sensor configurations were designed to solely measure knee Internal-External (IE) or Flexion-Extension (FE) rotations without STA [4,5].

Low efficiency of remote powering and limitation on electromagnetic emission are the main drawbacks of such internal measurement systems. The sensors cannot thus be powered on continuously. To reduce the power consumption a solution would be to use lower sampling rate and to duty cycle the sensors, turn them on just before each measurement and turn them off immediately after. However this could worsen the angle estimation.

The objective of this study was twofold. First we aimed to estimate both FE and IE rotation simultaneously by using an optimal sensor configuration of magnetic sensor in the knee implant. Second we used supplementary skin-mounted sensors to enhance the accuracy of low-sampled implantable magnetic sensors by a fusion operator.

METHODS

Angles estimation with implantable sensors- The implant used in this study (F.I.R.S.T, Symbios Switzerland) is a posterior-stabilized mobile-bearing knee prosthesis which consisted of a tibial part (TP), a femoral part (FP) and a polyethylene insert (PE). Based on almost conforming interface between FP and PE, we assumed that the IE rotation between FP and TP can be considered as the IE rotation between PE and TP [5]. Similarly FE rotation was considered as a rotation between FP and PE. Two magnets were fixed in TP and FP to convert their rotations to variations of magnetic flux passing through PE. A configuration of three 2D magnetic sensors (HMC1512, Honeywell USA) in PE was designed (Figure 1) to measure the defined FE and IE rotations. The best locations of sensors were obtained via sensitivity analyses on 10 different locations on a half of PE during FE and IE rotations. The knee prosthesis was fixed in a mechanical knee simulator equipped with reflective markers [5], in which we performed combinations of IE and FE rotations. A stereophotogrammetry system including four cameras (Vicon, UK) was synchronized with magnetic sensors, to provide the reference angles. The collected data at 200Hz was randomly sampled into 70% train and 30% test sets for 8 repeated times. These sets were used to train and evaluate the estimator performance. Each sensor measures a mixture of information from both angles. The IE and FE estimators

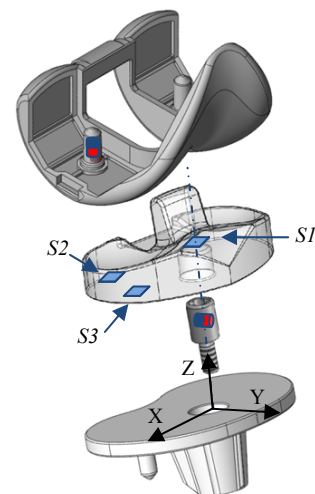


Figure 1: F.I.R.S.T prosthesis, with magnets and sensors configurations.

($\hat{\theta}_1^{IE}$, $\hat{\theta}_1^{FE}$) were linear regressions of selected inputs based on maximum correlation of sensors' measurements and the desired angle on train set so called forward selection [6]:

$$\hat{\theta}_1^{IE} = w_0 + w_1 S_{22} + w_2 S_{11} + w_3 (S_{22} \cdot S_{32}) \quad (1)$$

$$\hat{\theta}_1^{FE} = w_0 + w_1 S_{21} + w_2 S_{11} + w_3 (S_{21} \cdot S_{31}) + w_4 (S_{22} \cdot S_{32}) \quad (2)$$

where S_{ij} is the j^{th} channel measurements of i^{th} sensor and w_i is the linear regression coefficient obtained by employing least square criterion on train data set. Adding abduction-adduction (AA) movements via mechanical simulator during testing the estimators, we also studied their robustness.

Implantable/skin-mounted fusion to reduce power- The implanted sensors need average power of 69mW in continuous powering mode. At high sampling rate (200Hz) with duty cycling we can reduce it to 15mW. A sampling rate of 10Hz with duty cycling can drastically reduce the average power consumption to 2mW while the quality of signals is worsened. We proposed skin-mounted inertial sensors and a fusion algorithm to restore the quality of angle estimation. As long as the implantation on a subject has not done yet, the estimated knee angles via implantable sensors were simulated from fluoroscopic measurements on four subjects walking on treadmill. Angle estimations based on skin-mounted inertial sensors [7] were also simulated using skin markers and stereophotogrammetry motion capture. To simulate the internal measurements the worst case performance of estimators was used to generate random sequences of error which were added to reference measurements i.e. radio-stereometric analysis of the fluoroscopic measurements. Then, we down sampled the simulated measurements to 10Hz. Finally, the order weighted averaging (OWA) [8] was used as the fusion function (F_w). This computes a weighted sum of ordered angle estimators for every data point based on their errors on similar train samples, bigger weights are assigned to the better estimators:

$$F_w(\hat{\theta}_1, \hat{\theta}_2, \dots) = \sum_{i=1}^n w_i b_i \quad (3)$$

where b_i is the estimator with i^{th} lowest absolute error. The weights (w_i) were calculated via maximum entropy principle subject to OWA constraints and applied to the all samples.

RESULTS AND DISCUSSION

The best positions found for $S2$ and $S3$ were ($x=11$, $y=-11$, $z=2$) and ($x=9$, $y=4$, $z=2$) respectively (considering the coordinate frame in Figure 1), and $S1$ was best located at ($x=0$, $y=0$, $z=10$) all in millimeters. The performance of IE and FE angle estimators are shown in Table 1 (mean error: μ_e , error standard deviation: σ_e , coefficient of determination: R^2) for concurrent rotations. The reported value for each index is its expected value and standard deviation over 8 times repeated sampling on the collected data. This result manifests the capability of both estimators to extract IE and FE rotations' information from the mixed information of concurrent rotations. The estimators' performances show that AA artifact has an adverse effect on FE estimation but not a notable effect on IE estimation (Table 1).

The performance of simulated angles estimations and their OWA-based fusion are depicted in Table 2. The reported error indices are the expected values for average error and

standard deviation of error over all the subjects. Based on this result, the fusion drastically improved the FE angle estimation, but it does not enhance the IE estimation. In case of FE estimation the information is shared between the internal and external measurements. The former was STA-free but low-sampled and unsmooth, however the latter was blended with STA but smoother with higher sampling rate. The fusion thus provided improved angle estimations via combining the useful information from both systems. In contrast, having the internal estimation of IE, the external system does not bring any complementary information for this rotation because of STA. The fusion result on this angle was not thus better than internal estimation itself.

Table 1: Performance of angle estimators on test data sets in absence and presence of AA.

Estimators	Test data (30%)		
	μ_e (°)	σ_e (°)	R^2
$\hat{\theta}_1^{IE}$	-0.1 ± 0.2	0.9 ± 0.0	0.98 ± 0.01
$\hat{\theta}_1^{IE}$ (with AA)	0.0 ± 0.1	0.9 ± 0.0	0.97 ± 0.01
$\hat{\theta}_1^{FE}$	0.0 ± 0.8	3.4 ± 0.2	0.98 ± 0.00
$\hat{\theta}_1^{FE}$ (with AA)	-0.3 ± 1.1	4.3 ± 0.4	0.97 ± 0.01

Table 2: Simulated fusion results (in degree). Ex, Int and OWA are external, internal systems and fusion respectively.

Estimators	Test data (30%) over all 4 subjects		
	$\mu_e \pm \sigma_e$ (Ex) 200Hz	$\mu_e \pm \sigma_e$ (Int) 10Hz	$\mu_e \pm \sigma_e$ (OWA)
$\hat{\theta}_{simulated}^{IE}$	-2.3 ± 4.0	0.1 ± 0.8	0.0 ± 1.0
$\hat{\theta}_{simulated}^{FE}$	1.3 ± 4.8	3.4 ± 4.0	0.6 ± 3.2

CONCLUSIONS

Based on three magnetic sensors inserted in PE and two magnets in TP and FP of the knee prosthesis, two angle estimators were designed to measure accurately and concurrently FE and IE rotations in the presence of AA artifact. A method was proposed to lower the power consumption of the implantable sensors and to use information from skin-mounted sensors. The method was validated by simulation using worst case performance of the angle estimators, and the collected fluoroscopic and skin markers data of four subjects. It was shown that a low-sampled internal angle estimations fused with skin-mounted sensors through OWA improved FE angle estimation while the power consumption was significantly decreased.

ACKNOWLEDGEMENTS

The authors gratefully acknowledge the nano-Tera for funding the project (SNF20NAN1_123630).

REFERENCES

1. Kutzner I, et al., *J. Clin. Biomech.* **43**:2164-2173, 2010.
2. D'Lima DD, et al., *J. Clin. Ortho.* **466**: 2605-11, 2008.
3. Leardini A, et al., *Gait & Posture* **21**:212-225, 2005.
4. Arami A, et al., *J. IEEE T-ASE.* **10**, 2013.
5. Arami A, et al., *J. Biomech.* **45**: 2023-2027, 2012.
6. Nelles O, *Springer-Verlag*, 2001.
7. Favre J, et al., *J. Biomech.* **41**:1029-1035, 2008.
8. Yager R R, *IEEE Trans. SMC.* **18**: 183-190, 1988.